Stability of trapped Bose-Einstein condensate under a density-dependent gauge field

An-Qing Zhang, Chen Jiao, Zi-Fa Yu, Jie Wang, Ai-Xia Zhang, and Ju-Kui Xue*
College of Physics and Electronics Engineering, Northwest Normal University, Lanzhou 730070, China

(Received 9 August 2022; accepted 13 February 2023; published 27 February 2023)

We study the ground-state stability of the trapped one-dimensional Bose-Einstein condensate under a density-dependent gauge field by variational and numerical methods. The competition of density-dependent gauge field and mean-field atomic interaction induces the instability of the ground state, which results in irregular dynamics. The threshold of the gauge field for exciting the instability is obtained analytically and confirmed numerically. When the gauge field is less than the threshold, the system is stable, and the gauge field induces chiral dynamics of the wave packet. When the gauge field is greater than the threshold, the system is unstable, and the ground-state wave packet will be deformed and fragmented. Interestingly, we find that as the gauge field approaches the threshold, strong dipolar and breathing dynamics take place, and strong modes mixing occurs, the instability of the system sets in. In addition, we show that the stability of the system can be well controlled by periodical modulation of the trapping potential. We provide theoretical evidence to understand and control the irregular dynamics associated with chiral superfluid induced by density-dependent gauge field.

DOI: 10.1103/PhysRevE.107.024218

I. INTRODUCTION

The realization of Bose-Einstein condensate (BEC) has provided an ideal platform to probe some interesting physical phenomena under highly controllable conditions, for example, topological insulators [1], Hall effect [2], and nonlinear dynamics and solitons [3–6]. In particular, we can create synthetic gauge fields [7–9] for neutral atoms in the BEC system. The gauge field plays an important role in the BEC system. It can regulate the interaction between particles and influence many important physical phenomena, including spin-orbit coupling [10,11], the relativistic effect [12,13], Laughlin liquid [14], etc. These synthetic gauge fields can be introduced by Raman transition [15], lattice vibration [16,17], light-matter coupling [7], and laser-induced tunneling [9]. Such gauge fields are determined by external parameters such as the laser intensity or phase gradient of the incident laser field, and they are also uniformly distributed in space. These gauge fields are only described by the externally imposed time dependence [18], not by their own Hamiltonian, so they are all static gauge fields. In reality, the situation of the system should be more complex, so in order to make the gauge field nonuniformly distributed in space, and make this externally imposed time dependence transform into the system itself, it can be described by its own Hamiltonian: A dynamic gauge field is generated by the collisionally induced detuning for geometric potentials [19,20]. The time dependence of this gauge field does not depend on external parameters; it can be described by its own Hamiltonian. And this dynamic gauge field has been realized experimentally [21,22]. This gauge field changes with the variation of atomic density in space, and its distribution in space is nonuniform, which is also called a density-dependent gauge field.

With the increasing complexity of the BEC system, the research of nonlinear dynamics induced by density-dependent gauge field in BEC system has attracted extensive attention. This model breaks Galilean invariance and integrability, and can realize chiral solitons [23–26] in a one-dimensional BEC system. In particular, in the long time-scale limit, the wave function of trapped BEC system under the action of density-dependent gauge field has obvious deformation and delocalization compared with the initial state, which provides insights into the irregular dynamics associated with chiral superfluid [19,27–29] and unconventional vortex dynamics [20,30]. It is found that the density-dependent gauge field can strongly modify correlations in the superfluid regime. Furthermore, in the conventional condensed state without artificial gauge field, the collective oscillation of the system is ordinary, and the collective oscillation is harmonic with natural frequency. However, the collective dynamics of BEC with the gauge field is complex. The collective oscillation depends not only on the trapped potential and the interaction between atoms, but also on the strength of gauge field [12,31,32]. The nonlinear dynamics violates the dynamics of Kohn's theorem because the density-dependent gauge field breaks the Galilean invariance. When the intensity of gauge field is large, the dynamics is irregular. The density-dependent gauge field strongly modifies the dynamic characteristics of the system. Obviously, in BEC with a density-dependent gauge field, a quantum phenomenon induced by the gauge field is the irregular dynamics, which plays a role for the chiral superfluid. We expect that the origin of the irregular dynamics should be related to the instability of the system induced by the gauge field, which is an interesting and unsettled issue. The relationship between the irregular dynamics and collective dynamics is still an open subject.

*Corresponding author: xuejk@nwnu.edu.cn

In this paper, we study the ground-state stability and collective dynamics of trapped one-dimensional BEC under a density-dependent gauge field. Based on the variational analysis, the mechanism of irregular dynamics in the system is discussed. We find that the competition of density-dependent gauge field a and atomic interaction g induces ground-state instability, which results in irregular dynamics. The threshold of gauge field a_c for exciting the instability is obtained analytically, the stability diagram of the ground state determined by the gauge field, and the atomic interaction is presented. When $a < a_c$, the system is stable, the wave packet oscillates asymmetrically in the harmonic trap, and chiral oscillating dynamics occurs. In this case, the wave packet can preserve the Gauss-type profile. When $a > a_c$, the instability sets in, stable Gauss wave packet will not exist, and the wave packet will be deformed and fragmented. Further analysis shows that the instability is related to collective dynamics. The gauge field causes strong coupling between dipolar oscillation and breathing oscillation. In particular, when $a \to a_c$, the amplitudes of dipolar and breathing dynamics increase sharply, strong mode mixing takes place, and the system will be unstable. Interestingly, we find that the stability of the system is also closely related to the trapping potential and can be well controlled by periodically modulating the trapping potential. The analytical results are confirmed by numerical simulations.

The paper is organized as follows. In Sec. II, the mean field Gross-Pitaevskii equation (GPE) of trapped one-dimensional BEC under density-dependent gauge field is given. Then, using the variational method, we deduce the energy equation and the dynamical equations governing the center of mass and width of the wave packet. In Sec. III, the ground-state stability and collective dynamics of the system are discussed. In Sec. IV, strong mode mixing is presented. In Sec. V, the ground-state stability of the system is adjusted by periodically modulating the trapping potential. Section VI is our conclusion.

II. MODEL AND VARIATIONAL ANALYSIS

We consider a BEC consisting of N two-level atoms with internal states $|1\rangle$ and $|2\rangle$. The two internal states are coupled by a laser beam. The Hamiltonian of the system is written as [33]

$$\hat{H} = \left[\frac{\hat{\mathbf{p}}^2}{2m} + V(\mathbf{r})\right]\hat{I} + \hat{U} + \hat{\mathcal{V}}_{\text{int}}, \tag{1}$$

$$\hat{U} = \frac{\hbar}{2}\begin{pmatrix} 0 & \Omega e^{-i\phi_l} \\ \Omega e^{i\phi_l} & 0 \end{pmatrix}, \tag{2}$$

where $\hat{U}$ describes the light-matter interaction, Ω is the Raman frequency, ϕ_l is the laser phase, $V(\mathbf{r}) = \frac{1}{2}m\omega_{\mathbf{r}}^2\mathbf{r}^2$ is the trapped potential, and $\omega_{\mathbf{r}}$ is the frequency of the potential. The mean-field atomic interactions $\hat{\mathcal{V}}_{\text{int}} = \text{diag}[g_{11}|\Phi_1|^2 + g_{12}|\Phi_2|^2, g_{22}|\Phi_2|^2 + g_{12}|\Phi_1|^2]$, where $|\Phi_i|^2$ represents the atomic density in state $|i\rangle$. g_{ij} represents the coupling constant of the interaction between different components, which is related to the corresponding scattering length of $|i\rangle$ and $|j\rangle$ s waves between different components.

Under the condition of weak interaction, the frequency induced by detuning between atoms is much less than the Raman frequency. Then, the interaction between atoms can be regarded as a small disturbance of the interaction between light and matter. The eigenvalues of $\hat{U} + \hat{\mathcal{V}}_{\text{int}}$ can be obtained $|\chi_\pm\rangle = |\chi_\pm^{(0)}\rangle + |\chi_\pm^{(1)}\rangle$, where $|\chi_\pm^{(1)}\rangle = \pm[(g_{11} - g_{22})/(8\hbar\Omega)]$ $|\Phi_\pm|^2|\chi_\mp^{(0)}\rangle$. Its eigenvalue is $\tilde{g}|\Phi_\pm|^2 \pm \hbar\Omega/2$, where $\tilde{g} = (g_{11} + g_{22} + 2g_{12})/4$, $|\chi_\pm^{(0)}\rangle = [|1\rangle \pm e^{i\phi}|2\rangle]/\sqrt{2}$. Through the adiabatic approximation, the modified state can be used to represent the state vector $|\xi\rangle = \Sigma_{i=+,-}\Phi_i(\mathbf{r},t)|\chi_i\rangle$ of the system, and then the Hamiltonian of the system is written as

$$\hat{H}_\pm = \frac{(\hat{\mathbf{p}} - \mathbf{A}_\pm)^2}{2m} + W + \frac{\tilde{g}}{2}|\Phi_\pm|^2 + V(\mathbf{r}), \tag{3}$$

where $A_\pm = i\hbar\langle\chi_\pm|\nabla\chi_\pm\rangle$ is a vector potential and $W = \frac{\hbar^2}{2m}|\langle\chi_-|\nabla\chi_+\rangle|^2$ is a scalar potential. They come from the projection of the whole system on one of the dressed states. Then the gauge potential becomes $\mathbf{A}_\pm = \mathbf{A}^{(0)} \pm \tilde{\mathbf{a}}|\Phi_\pm|^2$, where $\mathbf{A}_0 = -\frac{\hbar}{2}\nabla\phi_l$ is the single-particle component and $\tilde{\mathbf{a}} = \nabla\phi_l(g_{11} - g_{22})/(8\Omega)$ is the effective intensity controlling the density-dependent vector potential. In order to derive the mean-field density-dependent Gross-Pitaevskii equation (GPE), we use the variational principle $\partial\pounds/\partial\Phi^* = 0$ to the action $\pounds = \langle\Phi|(i\hbar\frac{\partial}{\partial t} - \hat{H}_\pm)|\Phi\rangle$, with respect to Φ^*. We consider the branch of $+$ in $\hat{H}_\pm$, not loss of generality. The density-dependent GPE is obtained as

$$i\hbar\frac{\partial\Phi}{\partial t} = \left[\frac{1}{2m}(\hat{\mathbf{p}} - \hat{\mathbf{A}})^2 + W + V(\mathbf{r}) + \tilde{\mathbf{a}}\cdot\mathbf{J} + \tilde{g}|\Phi|^2\right]\Phi, \tag{4}$$

where $\mathbf{J}(\mathbf{r})$ is a nonlinear current, which describes a nonlinear gauge field,

$$\mathbf{J}(\mathbf{r}) = \frac{1}{2m}[\Phi(\hat{\mathbf{p}} + \hat{\mathbf{A}})\Phi^* - \Phi^*(\hat{\mathbf{p}} - \hat{\mathbf{A}})\Phi]. \tag{5}$$

We are interested in studying the dynamics and ground state of Eq. (4) in the one-dimensional framework. To achieve one dimension, we assume that the system is in the ground state of the transverse potential. In this way, we decompose the wave function into $\Phi(r,t) = \Psi_\perp(r_\perp)\Psi(x,t)$, $\Psi_\perp(r_\perp) = (\sqrt{\pi}l_\perp)^{-1}\exp(-r_\perp^2/2l_\perp^2)$ is the transverse ground-state wave function, and $l_\perp = \sqrt{\hbar/(m\omega_\perp)}$ is the transverse harmonic length scale. We define the laser phase as $\phi_l = kx$, and then eliminate the zero-order vector potential by momentum boost. Equation (4) is simplified to an effective one-dimensional form,

$$i\hbar\frac{\partial\Psi}{\partial t} = \left[\frac{1}{2m}(\hat{p} - \tilde{a}|\Psi|^2)^2 + \tilde{a}j(x) + W + g_{1D}|\Psi|^2\right]\Psi + V(x)\Psi, \tag{6}$$

where $V(x) = \frac{1}{2}m\omega_x^2x^2$. The effective gauge field strength $\tilde{a} = k(g_{11} - g_{22})/(16\pi\Omega l_\perp)$ and atomic interaction strength $g_{1D} = \tilde{g}/(2\pi l_\perp^2)$ are scaled according to the transverse area of the condensate, and the one-dimensional current nonlinearity is defined as

$$j(x) = \frac{1}{2m}[\Psi(p + \tilde{a}|\Psi|^2)\Psi^* - \Psi^*(p - \tilde{a}|\Psi|^2)\Psi]. \tag{7}$$

Equation (6) is further simplified by using nonlinear phase transformation $\Psi(x,t) = \psi(x,t)\exp[-i\phi_l/2 + i\tilde{a}\int_{-\infty}^{x}dx'|\Psi(x',t)|^2/\hbar - iWt/\hbar]$. When it is substituted into Eqs. (6)

and (7), the vector potential is decoupled from the canonical momentum, which leads to the simplified dimensionless equation

$$i\frac{\partial\psi}{\partial t} = \left[-\frac{1}{2}\frac{\partial^2}{\partial x^2} - ia\left(\psi\frac{\partial\psi^*}{\partial x} - \psi^*\frac{\partial\psi}{\partial x}\right) + g|\psi|^2\right]\psi + \frac{1}{2}\omega^2x^2\psi, \tag{8}$$

where the physical variables are rescaled as $\psi \to \sqrt{l_\perp}\psi$, $t \to t\omega_\perp$, $x \to x/l_\perp$. $g = g_{1D}/(\hbar\omega l_\perp)$, $a = \tilde{a}\hbar$, $\omega = \omega_x/\omega_\perp$. Equation (8) was originally studied under the background of one-dimensional anyons [34]. This GPE is nonintegrable, does not obey Galilean invariance, and has chiral soliton solutions. These properties can produce unconventional dynamics in the one-dimensional case. The effective Hamiltonian of Eq. (8) is

$$H = -\frac{1}{2}\frac{\partial^2}{\partial x^2} - ia\left(\psi\frac{\partial\psi^*}{\partial x} - \psi^*\frac{\partial\psi}{\partial x}\right) + g|\psi|^2 + \frac{1}{2}\omega^2x^2. \tag{9}$$

The collective dynamics and stability of condensate described by Eq. (8) are analyzed by a variational method. In order to explore the ground state and dynamic characteristics of the system, we use a Gaussian trial wave function

$$\psi(x,t) = (\sqrt{2\pi}R)^{-\frac{1}{2}}e^{-\frac{(x-x_0)^2}{2R^2}+ip(x-x_0)+\frac{i\delta}{2}(x-x_0)^2}. \tag{10}$$

The variational parameters are center of mass $x_0(t)$, width $R(t)$, chirp $\delta(t)$, and momentum $p(t)$ of the wave packet. The choice of a Gaussian ansatz is reasonable, since in the linear limit (without atomic interactions), it is precisely the ground state of the linear Schrödinger equation. Accordingly, for an interacting Bose gas, a natural and reasonable choice of the trial function is a Gaussian [35,36]. The reasonability of our analytical results obtained with Gaussian ansatz (10) is further well confirmed by numerical simulations of the full GPE Eq. (8). Substituting the trial wave function into the Lagrange equation

$$L = \int\left[\frac{i}{2}(\psi^*\dot{\psi} - \psi\dot{\psi}^*) - \psi^*H\psi\right]dx \tag{11}$$

and applying the Euler-Lagrangian equations $\partial L/\partial q_i - d(\partial L/\partial\dot{q}_i)/dt = 0$, where $q_i = \{x_0, R, p, \delta\}$, we obtain

$$\dot{x_0} = p - \frac{a\sqrt{\frac{2}{\pi}}}{R}, \tag{12}$$

$$\dot{\delta} = \frac{1}{R^4} + \frac{g - 4ap}{\sqrt{2\pi}R^3} - \delta^2 - \omega^2, \tag{13}$$

$$\dot{R} = R\delta, \tag{14}$$

$$\dot{p} = -\omega^2x_0. \tag{15}$$

Then, the energy of the system $E = \int\psi^*H\psi dx$ can be obtained:

$$E = \frac{1}{4R^2} + \sqrt{\frac{1}{8\pi}}\frac{g}{R} - \frac{a^2}{\pi R^2} + \frac{1}{4}\omega^2R^2. \tag{16}$$

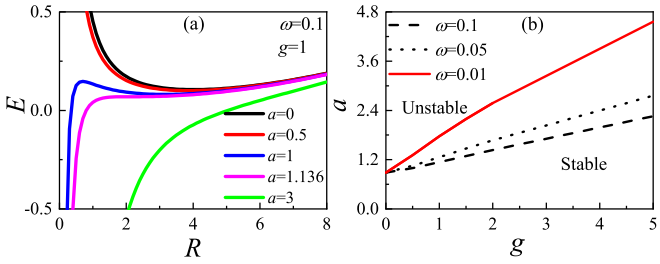

FIG. 1. (a) Energy E against R. (b) Stability diagram of ground state in (g, a) plane under different trapping potential.

The ground state and the dynamics of the system can be described by Eqs. (12) and (16).

III. STABILITY OF GROUND STATE

The energy in Eq. (16) corresponds to the kinetic energy, the atomic interaction energy, the coupling energy induced by the gauge field (nonlinearity current), and the potential energy, respectively. Here, we consider repulsive atomic interaction, i.e., $g > 0$. In particular, the energy term induced by gauge field is negative and is scaled as $-R^{-2}$, which is analogous to the one resulted from the attractive cubic nonlinearity of usual 2D GPE [37,38]. The two-dimensional (2D) GPE with attractive cubic nonlinearity suffers from collapse instability, i.e., $E \to -\infty$ as $R \to 0$. Hence, we conclude that the density-dependent gauge field should induce instability of the Gauss wave packet (collapse like instability). As shown in Fig. 1(a), for fixed atomic interaction g, there is a threshold of the gauge field strength, $a = a_c$; when $a < a_c$, the energy E has a minimum and the Gauss wave packet should be stable, while for $a > a_c$, an energy minimum does not exist and $E \to -\infty$ as $R \to 0$, the wave packet should be unstable. The threshold of the gauge field strength a_c can be obtained analytically according to Eqs. (12)–(16).

Setting $\dot{q}_i = 0$, the corresponding steady state of Eqs. (12)–(15) can be obtained,

$$-\sqrt{2\pi}\omega^2R_0^4 + \sqrt{2\pi} + gR_0 - 4a^2\sqrt{\frac{2}{\pi}} = 0, \tag{17}$$

with $p = \frac{a\sqrt{\frac{2}{\pi}}}{R}$, $x_0 = 0$, and $\delta = 0$. Therefore, once we know R_0 and p, the existence of the steady state of the condensate can be checked.

Now we discuss the threshold of instability induced by density-dependent gauge field. For a stable ground state, the state with the lowest energy should be selected, and the eigenvalue of the Hessian matrix must be positive. Therefore, R must satisfy $\partial E/\partial R = 0$ [i.e., Eq. (17)] and $\partial^2E/\partial^2R > 0$, which results in

$$a < a_c = \frac{1}{4}\left(\sqrt{\frac{5\pi}{2}}gR_0 + 4\pi\right)^{\frac{1}{2}}, \tag{18}$$

where R_0 is determined by Eq. (17). Equation (18) is one of our key results. The density-dependent gauge potential results in the instability of the system. When $0 \leqslant a < a_c$, the system is stable with repulsive atomic interaction. However, even with repulsive atomic interaction, the system can be unstable

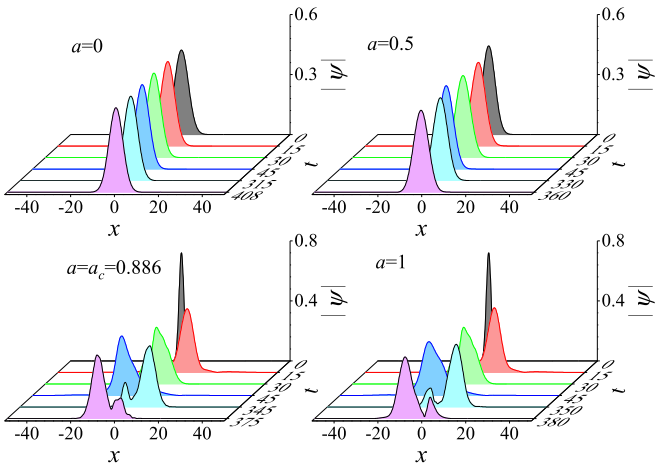

FIG. 2. Time evolution of wave packet with different density-dependent gauge field a at $\omega = 0.1$, $g = 0$.

when the current nonlinearity induced by density-dependent gauge potential is stronger, i.e., $a > a_c$. In this case, the stable Gauss wave packet will not exist, and the wave packet will be deformed and fragmented. The stability phase diagram of the ground state determined by density-dependent gauge field strength a and atomic interaction g can be obtained, which is shown in Fig. 1(b). It is clear that a_c increases (decreases) with $g(\omega)$. That is, strong (weak) repulsive atomic interaction (trapping potential) can prevent the instability induced by the gauge potential. Interestingly, when $g = 0$, a_c is independent of the trapping potential ω. The density-dependent gauge potential, the atomic interaction, and the trapping potential have coupled effects on the stability of the system.

To confirm the variational prediction given in Fig. 1, by using the fourth-order Runge-Kutta method, direct numerical simulations of Eq. (8) are provided and some results are shown in Figs. 2 and 3. Under the small displacement of the center-of-mass of the wave packet from the steady state $x_0 = 0$, i.e., $\Delta x_0 = 0.5$, $\Delta R_0 = 0$, Figs. 2 and 3 show the wave packet dynamics with different a for $g = 0$ and $g = 1$, respectively. The dipolar oscillation of wave

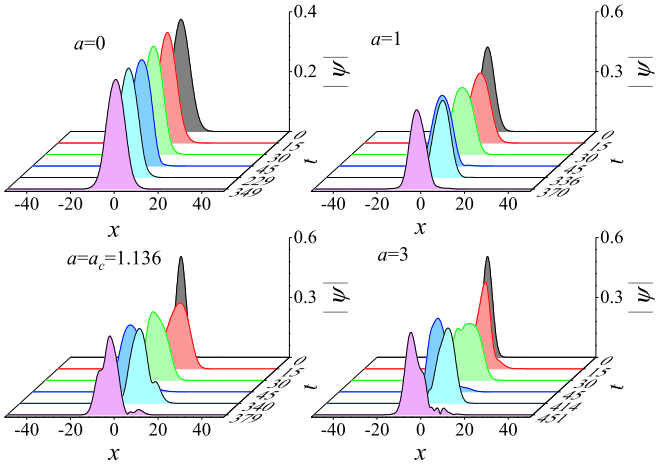

FIG. 3. Time evolution of wave packet with different density-dependent gauge field a at $\omega = 0.1$, $g = 1$.

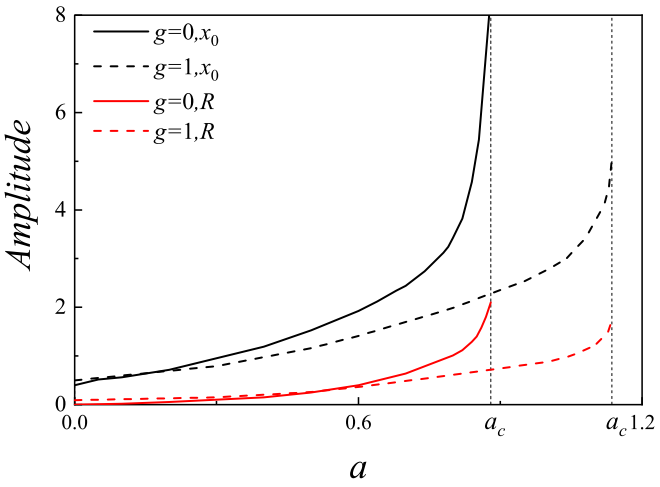

FIG. 4. The dipolar (black line) and breathing (red line) oscillation amplitude as a function of a for $\omega = 0.1$, $g = 0$ (solid line), and $g = 1$ (dashed line).

packet is excited. We find, when $a < a_c \simeq 0.886$ in Fig. 2 ($a < a_c \simeq 1.136$ in Fig. 3), the wave packet preserves the stable Gauss-type profile. When $a \geqslant a_c$, the wave packet cannot preserve the stable Gauss-type profile and the wave packet is deformed and fragmented. The instability of the system sets in. Figures 2 and 3 confirm the variational predictions. When the gauge potential does not exist ($a = 0$), the wave packet oscillates symmetrically in the harmonic trap without deformation. However, when the gauge potential is introduced and as a increases ($0 < a < a_c$), the wave packet oscillates asymmetrically, the wave front (wave rear) is compressed (broadened) when it moves left or right from its steady-state position, and preserves its symmetry when it returns to the initial position. Chiral dynamics is excited. With the increase of repulsive atomic interaction g (Fig. 3), this phenomenon becomes more obvious. The chiral nonlinear current induced by the density-dependent gauge potential results in this asymmetry dynamics. The nonlinear current is a spatial function and changes sign when the wave packet oscillates in the harmonic trap. The successive changing of the sign of current nonlinearity results in focusing and defocusing effects, which results in the asymmetric dynamics of the wave packet. When $a > a_c$, the current nonlinearity dominates over the atomic interaction. Then, the strong successive asymmetric oscillation dynamics results in the deformation of wave packet. The instability is excited.

The deformation and instability of wave packets can also be understood by the strong dipolar dynamics and the coupling of dipolar and breathing dynamics. Figures 2 and 3 show that as a increases, the amplitude of the center-of-mass of the wave packet increases significantly and the breathing dynamics is also excited, indicating that the dipolar and breathing dynamics are strongly coupled. This is further clearly shown in Figs. 4 and 5. When $a = 0$, the breathing dynamics is not excited (see the third row in Fig. 5, where $R \equiv R_0$). When $a > 0$, R oscillates around R_0, and the breathing dynamics is excited. Particularly, when $a \to a_c$, the amplitudes of dipolar and breathing oscillation increase sharply (Fig. 4), and the oscillation of the width of the wave packet is irregular (see

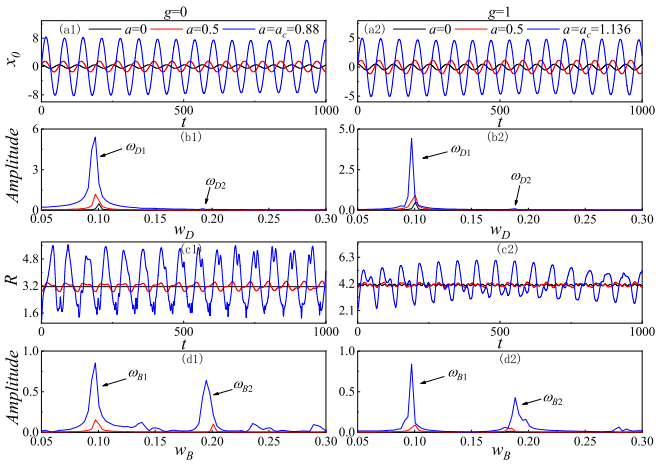

FIG. 5. [(a1), (a2), (c1), (c2)] Time evolution of the center-of-mass and width of wave packet with different g and a, respectively. [(b1), (b2), (d1), (d2)] Corresponding spectrum analysis. $\omega = 0.1$.

the third row in Fig. 5). Accordingly, the stable dipolar and breathing dynamics are broken. The strong dipolar dynamics accompanied by strong coupling of dipolar dynamics and breathing dynamics result in strong mode mixing, which induces the instability of the Gauss wave packet, and the wave packet will be deformed and fragmented. The dipolar dynamics shown in Fig. 5 (the first row) also shows a chirality: When $a = 0$, the wave packet moves to the negative x_0 direction from its initial position when $t > 0$, while for $a > 0$, the wave packet moves from the initial position to the positive x_0 direction when $t > 0$. The motion direction of the wave packet is changed by the gauge potential.

The strong mode mixing induced by the gauge field at $a = a_c$ is particularly obvious for breathing dynamics (see the third and fourth rows of Fig. 5), where the breathing dynamics is irregular (the third row in Fig. 5) and many modes are excited (the fourth row in Fig. 5). Correspondingly, the wave packet is deformed at $a = a_c$. The spectrum analysis in Fig. 5 indicates that the two main dipolar (breathing) modes are $\omega_{D1,2}$ ($\omega_{B1,2}$). The dipolar oscillation is dominated by the lower mode ω_{D1}, while the breathing oscillation is the nearly equal superposition of the lower (ω_{B1}) and higher (ω_{B2}) modes. When $a \to a_c$, the amplitude of collective modes increases sharply. Importantly, one can find $\omega_{D1} = \omega_{B1}$ and $\omega_{D2} = \omega_{B2}$ when $a > 0$. That is, the density-dependent gauge field induces the complete coupling of dipolar and breathing dynamics.

IV. STRONG MODES MIXING

The strong dipolar dynamics and breathing dynamics shown in Figs. 2–5 can be well understood by the time-dependent variational analysis. The motion equations of collective dynamics (12)–(15) can be deduced to

$$\ddot{x_0} + \omega^2 x_0 - \frac{a\sqrt{\frac{2}{\pi}}}{R^2}\dot{R} = 0, \tag{19}$$

$$\ddot{R} - \frac{1}{R^3} - \frac{g - 4a\dot{x_0}}{\sqrt{2\pi}R^2} + \frac{4a^2\sqrt{\frac{2}{\pi}}}{\sqrt{2\pi}R^3} + \omega^2 R = 0. \tag{20}$$

Equations (19) and (20) describe the dipolar and breathing dynamics, which are coupled by the density-dependent gauge field a. The dynamics of the system is fundamentally different from that of the conventional BEC system. Equation (19) describing the dipolar dynamics of the system no longer only depends on the trapped potential, but has a nonlinear term caused by the density-dependent gauge field. Moreover, Eq. (20) describing the breathing dynamics of the system also has two additional terms, which are proportional to the velocity of the center of mass and the strength of the gauge field. Because of the existence of density-dependent gauge field, dipolar dynamics and breathing dynamics are coupled with each other. Collective oscillation can be regarded as the superposition between dipolar mode and breathing mode, which leads to the emergence of a harmonic collective behavior. To obtain the collective modes analytically, we consider the weak perturbation of equilibrium states q_{i0}. Inserting $q_i = q_{i0} + \delta q_{i0}$ into Eqs. (19) and (20), we obtain the linearized equation of collective dynamics:

$$\delta\ddot{x_0} + \omega^2\delta x_0 - A_{11}\delta\dot{R} = 0, \tag{21}$$

$$\delta\ddot{R} + (A_{21} + \omega^2)\delta R + A_{22}\delta\dot{x_0} = 0, \tag{22}$$

where $A_{11} = a\sqrt{2/\pi}/R_0^2, A_{21} = 3/R_0^4 + 2g/(\sqrt{2\pi}R_0^3) - 12a^2\sqrt{2/\pi}/(\sqrt{2\pi}R_0^4), A_{22} = 4a/(\sqrt{2\pi}R_0^2)$. According to Eqs. (21) and (22), we obtain

$$\delta\dddot{x_0} + [2\omega^2 + A_{21} + A_{11}A_{22}]\delta\ddot{x_0} + (A_{21} + \omega^2)\delta x_0 = 0, \tag{23}$$

where $\delta\dddot{x_0}$ is the fourth-order derivative respective to t. The dipolar frequency can be obtained from the characteristic equation of Eq. (23):

$$\omega_{D1,2} = \frac{1}{\sqrt{2}}\left[\frac{1}{R_0^4} + 4\omega^2 \mp \sqrt{\left(\frac{1}{R_0^4} + 2\omega^2\right)^2 + \frac{16a^2\omega^2}{\pi R_0^4}}\right]^{\frac{1}{2}}, \tag{24}$$

and the dipolar oscillation can be described as

$$x_0 = A_{D1}\cos(\omega_{D1}t) + A_{D2}\cos(\omega_{D2}t), \tag{25}$$

where $A_{D1,2} = \pm[(\omega^2 - \omega_{D2,1}^2)/(\omega_{D1}^2 - \omega_{D2}^2)]\Delta x_0$, and Δx_0 is the initial displacement of the center-of-mass from the equilibrium position. Because of the coupling effect of gauge field, the breathing dynamics excited by the dipolar oscillation can be obtained,

$$R = R_0 + A_{B1}\sin(\omega_{D1}t) + A_{B2}\sin(\omega_{D2}t), \tag{26}$$

where $A_{B1} = A_{D1}(\omega^2 - \omega_{D1}^2)/(A_{11}\omega_{D1}), A_{B2} = A_{D2}(\omega^2 - \omega_{D2}^2)/(A_{11}\omega_{D2})$. From the above results, it is found that the dipolar frequency is the same as the breathing frequency due to the coupling effect of the gauge field, which is in good agreement with the numerical results shown in Fig. 5.

The collective frequencies and their amplitudes are shown in Fig. 6. One finds from Fig. 6(a) that the lower mode (ω_{D1}, ω_{B1}) decreases (increases) with $a(g)$, while the higher mode (ω_{D2}, ω_{B2}) increases (decreases) with $a(g)$. Importantly, the amplitude of the lower dipolar mode is far larger than that of the higher dipolar mode, i.e., $A_{D1} \gg A_{D2}$ [see Fig. 6(b)], which means the lower dipolar mode is dominant. That is,

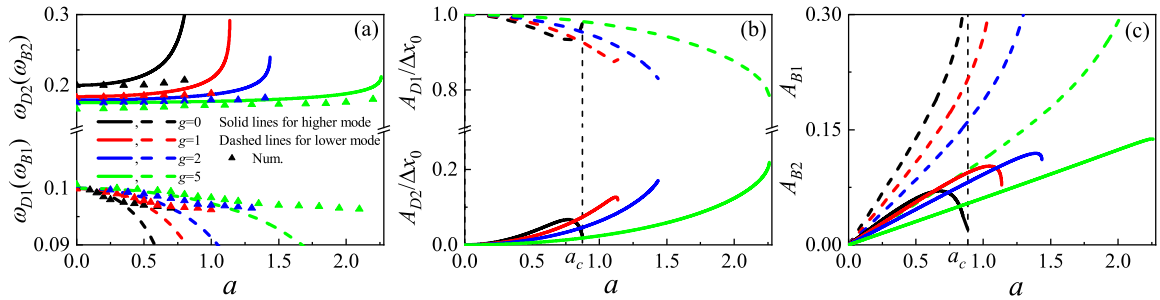

FIG. 6. (a) The oscillation frequencies corresponding to dipolar oscillation and breathing oscillation. The line is the analytical result given by Eq. (24), while the triangle is the numerical result. (b) The amplitude corresponding to the dipolar oscillation. (c) The amplitude corresponding to the breathing oscillation. In all figures, the solid (dashed) lines refer to the variables of higher (lower) collective mode. $\omega = 0.1$.

the dipolar oscillation is harmonic with the lower dipolar mode ω_{D1}. This is consistent with numerical results shown in the first and second rows of Fig. 5. For the breathing mode, however, the amplitudes of the two modes (A_{B1}, A_{B2}) are in same order and increase with a [see Fig. 6(c)]. That is, the breathing oscillation is the superposition of the two external modes excited by dipolar dynamics, which is enhanced significantly as a increases. The coupling of two (even more) external modes induces irregular breathing dynamics, which results in the instability of the wave packet. This is confirmed by numerical simulations (see the third and fourth rows in Fig. 5). When $a = 0$, the dipolar oscillation is harmonic with inherent frequency $\omega_D = \omega$, i.e., $A_{D1} = 1$ and $A_{D2} = 0$. The amplitude corresponding to the other external mode is zero. In this case, the dipolar dynamics and the breathing dynamics are decoupled, so the breathing dynamics does not excited, $A_{B1,2} = 0$. The variational results are consistent with the results of numerical simulation (see Fig. 5). We provide theoretical evidence to understand the irregular dynamics induced by density-dependent gauge field.

Note that, as shown in Fig. 6(a), the collective frequencies predicted by the analytical result and direct numerical simulation are in good agreement when the gauge field is weak, while for $a \to a_c$, the collective frequencies obtained by the two methods are inconsistent. The reason is that the analytical result given by Eq. (24) is obtained by linearization method, which should hold for weak excitation (i.e., with small amplitude oscillation). However, as shown in Fig. 4, when $a \to a_c$, the effect of nonlinear current is enhanced significantly, the amplitude of collective dynamics increases sharply, and strong nonlinear modes mixing occurs, which cannot be captured by linearization method. Strong atomic interaction can prevent the instability induced by the gauge potential. Figure 6 shows that as g increases, the validation of the collective frequencies predicted by linearization is improved obviously.

V. PERIODIC MODULATION

The previous sections show that the density-dependent gauge field induced instability of wave packets depends on the intensity of gauge field, atomic interaction, and the trapping potential, and remarkable results are obtained.

In order to better control the stability of the ground state, we perform periodical modulation of the trapping potential and then adjust the stability of the condensate. We consider the system described by Eq. (8),

$$i\frac{\partial\psi}{\partial t} = (H_0 + H_I)\psi, \tag{27}$$

shere $H_0 = [-\frac{1}{2}\frac{\partial^2}{\partial x^2} - 2aj(x)] + V(x,t)$ and $H_I = g|\psi|^2$. We assume that the trapping potential changes periodically with time

$$V(x,t) = \tfrac{1}{2}x^2\omega^2\cos(\Omega_0 t), \tag{28}$$

where Ω_0 is the modulation frequency, and this scheme can be easily realized by changing the frequency of the trapped potential [39]. The stability of ordinary 2D GPE with cubic self-attraction is studied by periodical modulation of the quadratic trapping potential and stable 2D fundamental-state modes under the action of the cubic self-attraction is predicted [40]. We assume that the modulation frequency Ω_0 is much larger than other energy scales in the system. Under this high-frequency condition, we can use the high-frequency approximation to offset the time-varying modulation term generated by the periodic modulation of the trapping potential. Therefore, we introduce unitary transformation [41] $\varphi = U^\dagger\psi$, $U = \exp[-i\sin(\Omega_0 t)x^2\omega^2/(2\Omega_0)]$, where the φ is the transformed wave function. Then, according to Floquet theory, the transformed Hamiltonian can be written as

$$H' = U^\dagger(H_0 + H_I)U - iU^\dagger\frac{\partial U}{\partial t}. \tag{29}$$

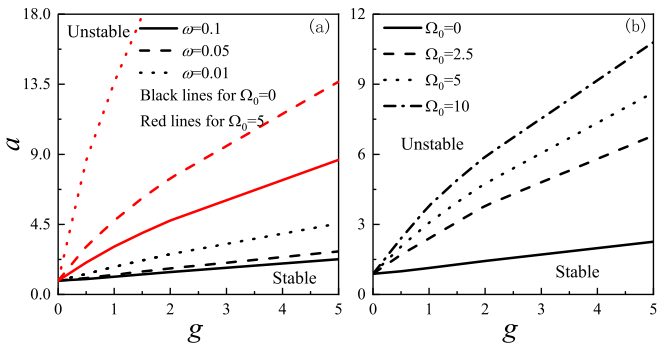

FIG. 7. The stability diagram of ground state under different parameters: (a) for different ω with $(\Omega_0 = 5)$ and without $(\Omega_0 = 0)$ modulation, (b) for different Ω_0 with $\omega = 0.1$.

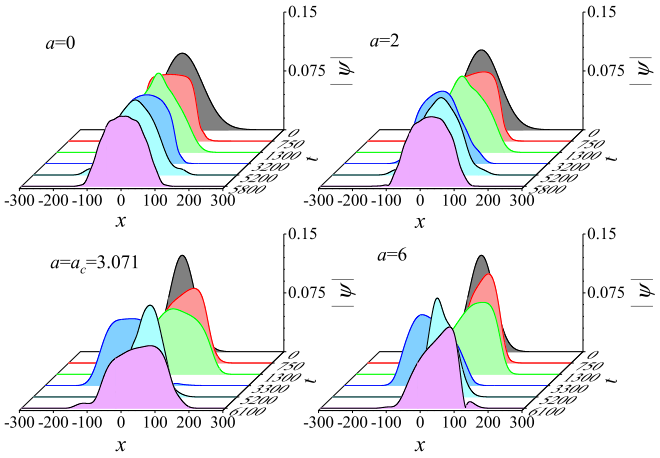

FIG. 8. Time evolution of wave packet with different a under periodic modulation. $\omega = 0.1$, $\Omega_0 = 5$, $g = 1$.

In order to obtain the time-independent Hamiltonian, we eliminate the time-varying part of the transformed Hamiltonian by the following integral, $\bar{H} = \int_0^\tau H' dt = \bar{H}_0 + \bar{H}_I$, where $\tau = 2\pi/\Omega_0$ is the modulation period, $\bar{H}$ is a time-independent Hamiltonian, $\bar{H}_0$ is an effective single-particle Hamiltonian, and $\bar{H}_I$ is the Hamiltonian of atomic interaction, and then the effective Hamiltonian becomes

$$\bar{H} = \left[-\frac{1}{2}\frac{\partial^2}{\partial x^2} - 2aj(x)\right] + \frac{1}{2}\Omega_1^2 x^2 + g|\varphi|^2,$$
$$j(x) = \frac{i}{2}\left[\varphi\frac{\partial\varphi^*}{\partial x} - \varphi^*\frac{\partial\varphi}{\partial x}\right], \tag{30}$$

where $\Omega_1 = \omega^2/(\sqrt{2}\Omega_0)$ is the effective trapping potential. Under the trial wave function (10), the energy of the system is

$$E = \frac{1}{4R^2} + \sqrt{\frac{1}{8\pi}}\frac{g}{R} - \frac{a^2}{\pi R^2} + \frac{1}{4}\Omega_1^2 R^2. \tag{31}$$

Comparing Eq. (8) [or Eq. (16)] with Eq. (30) [or Eq. (31)], the modulation of external trapping potential only results in modification of the frequency of the trapping potential; i.e., ω is changed to $\Omega_1 = \omega^2/(\sqrt{2}\Omega_0)$. The modulation weakens the external trapping. As shown in Fig. 1, a weak trapping potential can prevent the instability induced by the gauge field. Then, we conclude that the periodic modulation of the external trapping potential can enhance the stability of the system. Replacing ω with Ω_1, the stability diagram of the modulated system can be obtained according to Eqs. (17) and (18), which is shown in Fig. 7. For fixed ω, the stable region can be significantly expanded with modulation ($\Omega_0 \neq 0$) [Fig. 7(a)] and the stable region increases with Ω_0 [Fig. 7(b)].

The periodic modulation of the trapping potential can prevent the instability induced by the density-dependent gauge potential. The results of the numerical simulation of Eq. (27) are shown in Fig. 8, which confirms our variational predictions. We find that when $a = 0$, the wave packet oscillates symmetrically without any deformation. When $0 < a < a_c = 3.071$, the wave packet oscillates asymmetrically, and significant chiral dynamics takes place. That is, the chirality of the wave packet is enhanced by modulation. The reason is that under periodic modulation, the trapping effect on the condensate decreases, and the oscillation of the ground-state wave packet becomes more active, which further suppresses the instability caused by the gauge potential. Therefore, the chirality of the ground-state wave packet under periodic modulation is stronger than that without periodic modulation. When $a > a_c$, the wave packets are deformed, and instability is excited. Periodic modulation of external trapping potential provides a mechanism for controlling the topological and chiral properties of condensates with a density-dependent gauge field.

VI. CONCLUSIONS

In conclusion, using variational analysis and numerical simulation, the stability of trapped one-dimensional Bose-Einstein condensate under density-dependent gauge field is studied. The physical mechanism for exciting the instability and irregular dynamics of the system is revealed and some interesting phenomena are predicted. The competition between density-dependent gauge field and mean-field atomic interaction induces instability and irregular dynamics. The threshold for exciting the instability is obtained analytically and confirmed numerically. When the atomic interaction is dominant, stable chiral Gaussian wave packet dynamics is observed. However, when the gauge field is dominant, strong coupling of dipolar and breathing dynamics takes place, the system is unstable, and the wave packet will be deformed and fragmented. Interestingly, the stability of the system can be adjusted by periodically modulating the trapping potential.

ACKNOWLEDGMENTS

This work is supported by the National Natural Science Foundation of China under Grants No. 12164042, No. 12264045, No. 11764039, No. 11847304, No. 11865014, and No. 11475027; by Natural Science Foundation of Gansu Province under Grant No. 17JR5RA07620JR5RA526; by a scientific research project of Gansu Higher Education under Grant No. 2016A-005; by Innovation Capability Enhancement Project of Gansu Higher Education under Grants No. 2020A-146 and No. 2019A-014; and by Creation of Science and Technology of Northwest Normal University under Grant No. NWNU-LKQN-18-33.

[1] M. Z. Hasan and C. L. Kane, Rev. Mod. Phys. **82**, 3045 (2010).
[2] D. C. Tsui, H. L. Stormer, and A. C. Gossard, Phys. Rev. Lett. **48**, 1559 (1982).
[3] S. Burger, K. Bongs, S. Dettmer, W. Ertmer, K. Sengstock, A. Sanpera, G. V. Shlyapnikov, and M. Lewenstein, Phys. Rev. Lett. **83**, 5198 (1999).
[4] J. Denschlag, J. E. Simsarian, and D. L. Feder, Science **287**, 97 (2000).
[5] G. J. Dong, J. Zhu, W. P. Zhang, and B. A. Malomed, Phys. Rev. Lett. **110**, 250401 (2013).
[6] Z. X. Liang, Z. D. Zhang, and W. M. Liu, Phys. Rev. Lett. **94**, 050402 (2005).

[7] Y. J. Lin, R. L. Compton, K. J. García, J. V. Porto, and I. B. Spielman, Nature (London) **462**, 628 (2009).
[8] R. A. Williams, L. J. LeBlanc, K. J. Garcia, M. C. Beeler, A. R. Perry, W. D. Phillips, and I. B. Spielman, Science **335**, 314 (2012).
[9] M. Aidelsburger, M. Atala, S. Nascimbéne, S. Trotzky, Y.-A. Chen, and I. Bloch, Phys. Rev. Lett. **107**, 255301 (2011).
[10] Y. J. Lin, K. J. García, and I. B. Spielman, Nature (London) **471**, 83 (2011).
[11] P. Wang, Z. Q. Yu, Z. Fu, J. Miao, L. Huang, S. Chai, H. Zhai, and J. Zhang, Phys. Rev. Lett. **109**, 095301 (2012).
[12] M. Merkl, F. E. Zimmer, G. Juzeliunas, and P. Öhberg, Europhys. Lett. **83**, 54002 (2008).
[13] J. Ruseckas, G. Juzeliūnas, P. Öhberg, and M. Fleischhauer, Phys. Rev. Lett. **95**, 010404 (2005).
[14] R. B. Laughlin, Phys. Rev. Lett. **50**, 1395 (1983).
[15] Y. J. Lin, R. L. Compton, A. R. Perry, W. D. Phillips, J. V. Porto, and I. B. Spielman, Phys. Rev. Lett. **102**, 130401 (2009).
[16] K. W. Madison, F. Chevy, W. Wohlleben, and J. Dalibard, Phys. Rev. Lett. **84**, 806 (2000).
[17] J. Struck, C. Ölschläger, M. Weinberg, P. Hauke, J. Simonet, A. Eckardt, M. Lewenstein, K. Sengstock, and P. Windpassinger, Phys. Rev. Lett. **108**, 225304 (2012).
[18] Y. J. Lin, R. L. Compton, K. J. Garcia, W. D. Phillips, J. V. Porto, and I. B. Spielman, Nat. Phys. **7**, 531 (2011).
[19] M. J. Edmonds, M. Valiente, and P. Öhberg, Europhys. Lett. **110**, 36004 (2015).
[20] S. Butera, M. Valiente, and P. Öhberg, New J. Phys. **18**, 085001 (2016).
[21] E. A. Martinez, C. A. Muschik, P. Schindler, D. Nigg, A. Erhard, M. Heyl, P. Hauke, M. Dalmonte, T. Monz, P. Zoller, and R. Blatt, Nature (London) **534**, 516 (2016).
[22] L. W. Clark, B. M. Anderson, L. Feng, A. Gaj, K. Levin, and C. Chin, Phys. Rev. Lett. **121**, 030402 (2018).
[23] R. J. Dingwall, M. J. Edmonds, J. L. Helm, B. A. Malomed, and P. Öhberg, New J. Phys. **20**, 043004 (2018).
[24] R. J. Dingwall and P. Öhberg, Phys. Rev. A **99**, 023609 (2019).
[25] M. J. Edmonds, M. Valiente, G. Juzeliūnas, L. Santos, and P. Öhberg, Phys. Rev. Lett. **110**, 085301 (2013).
[26] R. Gao, X. Qiao, Y. E. Ma, Y. Jian, A. X. Zhang, and J. K. Xue, Phys. Lett. A **446**, 128283 (2022).
[27] M. Saleh and P. Öhberg, J. Phys. B **51**, 045303 (2018).
[28] L. Chen and Q. Zhu, New J. Phys. **24**, 053044 (2022).
[29] I. A. Bhat, S. Sivaprakasam, and B. A. Malomed, Phys. Rev. E **103**, 032206 (2021).
[30] M. Edmonds and M. Nitta, Phys. Rev. A **102**, 011303(R) (2020).
[31] J. Y. Zhang, S. C. Ji, Z. Chen, L. Zhang, Z. D. Du, B. Yan, G. S. Pan, B. Zhao, Y. J. Deng, H. Zhai, S. Chen, and J. W. Pan, Phys. Rev. Lett. **109**, 115301 (2012).
[32] Y. Zhang, L. Mao, and C. Zhang, Phys. Rev. Lett. **108**, 035302 (2012).
[33] N. Goldman, G. Juzeliūnas, P. Öhberg, and I. B. Spielman, Rep. Prog. Phys. **77**, 126401 (2014).
[34] U. Aglietti, L. Griguolo, R. Jackiw, S. Y. Pi, and D. Seminara, Phys. Rev. Lett. **77**, 4406 (1996).
[35] V. M. Pérez-García, H. Michinel, J. I. Cirac, M. Lewenstein, and P. Zoller, Phys. Rev. Lett. **77**, 5320 (1996).
[36] V. M. Pérez-García, H. Michinel, J. I. Cirac, M. Lewenstein, and P. Zoller, Phys. Rev. A **56**, 1424 (1997).
[37] I. Tikhonenkov, B. A. Malomed, and A. Vardi, Phys. Rev. Lett. **100**, 090406 (2008).
[38] Y. C. Zhang, Z. W. Zhou, B. A. Malomed, and H. Pu, Phys. Rev. Lett. **115**, 253902 (2015).
[39] C. F. Foot, *Atomic Physics* (Oxford University Press, New York, 2005).
[40] Z. H. Luo, Y. Liu, Y. Y. Li, J. Batle, and B. A. Malomed, Phys. Rev. E **106**, 014201 (2022).
[41] Y. Zhang, G. Chen, and C. Zhang, Sci. Rep. **3**, 1937 (2013).